ELSEVIER

Journal of Power Sources 54 (1995) 356–361

JOURNAL OF POWER SOURCES

Cyclic voltammetric and Raman spectroscopic studies of the $Li/LiAlCl_4/SO_2$ and $Li/LiGaCl_4/SO_2$ rechargeable systems

M. Goledzinowski, R.J. Doré, I.R. Hill *

Electrochemical Science and Technology Centre, University of Ottawa, 33 Mann Avenue, Ottawa, Ont., K1N 6N5, Canada

Abstract

Cyclic voltammetry was used to follow the electrochemical properties of $LiAlCl_4$ and $LiGaCl_4$ dissolved in SO_2. The behaviour of the two electrolytes was very different indicating different reduction products at a glassy-carbon electrode. Attempts to identify the reduction products were made using in situ Raman spectroscopy of discharging $Li/LiMCl_4$, SO_2/C cells. Only the $LiGaCl_4$ electrolyte yielded a Raman spectrum. The species present was not lithium dithionite as is produced in non-rechargeable Li/SO_2 cells.

Keywords: Rechargeable lithium batteries; Aluminium; Gallium; Sulfur dioxide

1. Introduction

The lithium/sulfur dioxide primary battery system was discovered 25 years ago [1] and the possibility of rechargeability was suggested soon afterwards [2]. The primary batteries have: higher specific energy; higher power density; a longer shelf life, and can operate at lower temperatures than more conventional portable batteries. Development of a rechargeable Li/SO_2 system was documented by Schlaikjer [3] and Dey et al. [4], who introduced the use of an all-inorganic electrolyte of the form $LiAlCl_4 \cdot xSO_2$ where x is typically 2.8 to 6. The open-circuit voltage of this system is 3.2 V and the reduction products are thought to be LiCl and $LiAlCl(SO_2)_3$, the latter being complexed to carbon via the SO_2 species. In later work, chloroaluminates of Na, Ca, and Sr were used in order to improve the stability, conductivity and performance of the Li/SO_2 rechargeable system [5]. $LiGaCl_4 \cdot xSO_2$ has also been used which gives a lower cell open-circuit voltage, 2.9 V. Lithium tends to corrode in this electrolyte [6] and the cell discharge products are thought to be $Li_2S_2O_4$ [6,7], as with the primary system.

The objective of the present work was to compare the electrochemistry of cells containing $LiAlCl_4$ and $LiGaCl_4$. The nature of the cell discharge reactions will be discussed in the light of electrochemical and spectroscopic data.

2. Experimental

$LiAlCl_4$ and $LiGaCl_4$ were purchased from APL Engineered Materials Inc. (Urbana, IL) and used as-received. The electrolytes were prepared on a vacuum line by deliquescence with gaseous SO_2. A 4 mm diameter rod of glassy carbon sheathed in a glass tube was used as working electrode and lithium was used for both the counter and reference electrodes. The working electrode surface was polished using alumina/methanol. The cell was loaded inside a Vacuum Atmospheres glove box equipped with a Dri-Train. Electrochemical studies were performed in a glass cell held inside a Thermotron S4 environmental chamber. A PARC 273 potentiostat was used to make the electrochemical measurements. Raman spectroscopic measurements were performed with an Instruments SA HG2S spectrometer equipped with an argon ion laser and a cooled photomultiplier tube. Cell cycling was performed using an Arbin BT2020 automated battery test system.

* Corresponding author.

SSDI 0378-7753(94)02101-8

3. Results and discussion

3.1. Cyclic voltammetry studies

C/LiAlCl$_4$·xSO$_2$ system

Fig. 1 shows four of the first five cyclic voltammograms (CVs) for a glassy-carbon electrode in LiAlCl$_4$·3.0SO$_2$ at 20 °C, using a sweep rate of 100 mV s^{-1}. In the first cycle a reduction peak is seen at 2.9 V which passivates the electrode and is completely irreversible. A second weaker peak is seen at 2.4 V. In the positive sweep a weak peak is seen at 3.7 V, prior to chlorine evolution near 4.0 V. In the second and subsequent cycles, the 2.9 V peak is virtually absent and a weaker reduction peak is seen near 2.4 V. The reduction is evidently electrochemical-chemical in nature, whereby the products of the electrochemical reaction are chemically precipitated at the electrode surface. A plot of the 2.9 V peak current versus the square root of the sweep rate was found to yield a straight line, showing that the reduction was diffusion controlled. The CVs attained a steady state following five cycles with a reduction peak at 2.4 V and an oxidation peak at 3.7 V. The magnitude of the 3.7 V peak was found to decrease as the lower switching potential was progressively increased from 2.0 to 2.6 V. This showed that the 2.4 V/3.7 V peaks formed a redox couple. In addition, when the fresh glassy-carbon electrode was held at 3.0 V for various times up to 1 min before sweeping negatively for one cycle, the peaks at 2.4 and 3.7 V remained the same size. Assuming that the film following 1 min of holding at 3.0 V is thicker and less porous than that produced by sweeping at 100 mV s^{-1}, then the reduction taking place at 2.4 V must involve a species present in the film.

Fig. 2(A) compares single cycle voltammograms in LiAlCl$_4$·3SO$_2$ at 20 and 0 °C. The 2.9 V peak is weaker at 0 °C while the secondary reduction process at 2.4 V has not changed as much. In Fig. 2(B), single cycle voltammograms are compared for LiAlCl$_4$ electrolyte

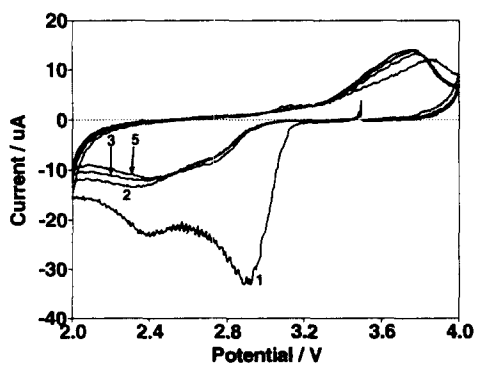

Fig. 1. Cyclic voltammograms obtained at a mechanically polished glassy-carbon electrode in LiAlCl$_4$·3.2SO$_2$, using a sweep rate of 100 mV s^{-1}. The numbers indicate the cycle number; 20 °C, lithium reference electrode.

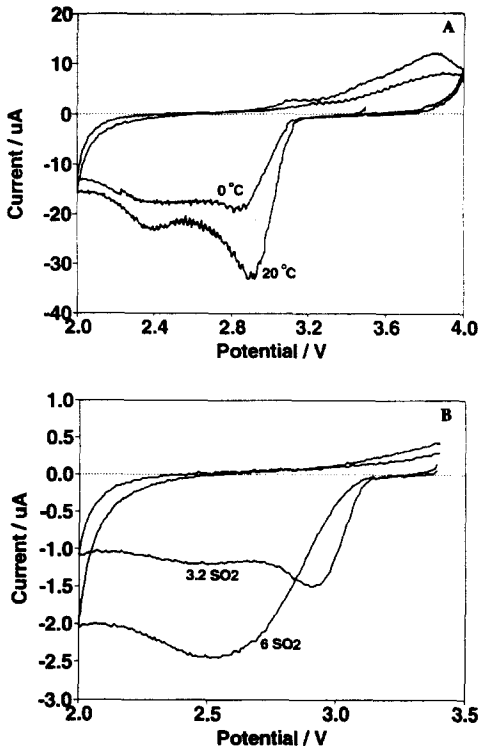

Fig. 2. A comparison of single-cycle voltammograms at mechanically polished glassy-carbon electrodes: (A) temperature dependence in the electrolyte LiAlCl$_4$·3.2SO$_2$ (sweep rate = 100 mV s^{-1}), and (B) concentration dependence at 0 °C when using LiAlCl$_4$·3.2SO$_2$ and LiAlCl$_4$·6SO$_2$ (sweep rate = 10 mV s^{-1}). A slower sweep rate was used in order to try and resolve a peak at 2.9 V.

at 0 °C containing 3.2 and 6.0 SO$_2$. A broad reduction peak is seen at about 2.4 V in 6.0 SO$_2$ electrolyte instead of the peak near 3.0 V. This means that the secondary reduction process at about 2.4 V is prevailing not only at lower temperatures but also for higher SO$_2$ content. It would appear that the reduction at 2.4 V involves SO$_2$. This also means that SO$_2$ should be present in the film produced at 2.9 V, in agreement with Dey et al. [4]. Although a reduction peak was observed at 2.4 V in cyclic voltammetry, no evidence of a plateau was seen at this voltage during the discharging of Li/LiAlCl$_4$·xSO$_2$/C (Ketjen black) cells. Therefore, the thick reduction film produced at 2.9 V during cell discharging must be too passivating to allow the reduction reaction at 2.4 V to take place.

The thickness of the primary deposit was estimated on the basis of the reduction charge. From cell cycling data, the discharging:charging efficiency is between 90 and 95%, so the majority of the discharge product must form a stable film on the carbon. For the purpose of the calculation it was assumed that Li$_2$S$_2$O$_4$ was the reduction product [8], since the objective was only to get the order of magnitude of the thickness and alternative reduction products would yield the same order of magnitude figures. The results of several experiments performed at room temperature using LiAlCl$_4$·3SO$_2$

were a film thickness of the order of 15 nm for the 2.9 V reduction peak. This shows that the species produced is more than just a single monolayer of complex adsorbed to carbon via SO_2.

3.1.2. $Li/LiGaCl_4 \cdot xSO_2/C$ system

It has been reported that the $Li/LiGaCl_4 \cdot xSO_2/C$ cell exhibits better conductivity and stability than the $Li/LiAlCl_4 \cdot xSO_2/C$ system in the temperature range from 0 to 40 °C [9]. Ga-containing cells were reported to yield a seven fold higher capacity than Al salt-based cells. We have used cyclic voltammetry to investigate these differences. This was carried out using $LiGaCl_4 \cdot 3.2SO_2$ and the results were very different from those using $LiAlCl_4$. Fig. 3(A) shows three consecutive cycles at 20 °C, using a sweep rate of 10 mV s^{-1}. The electrode clearly has not passivated as readily as in the case of $LiAlCl_4 \cdot 3SO_2$ so the reduction product may be slightly soluble. The peak current of the first cycle is about two orders of magnitude larger than that seen with $LiAlCl_4$: the charge passed was approximately 70 times larger. The peak potential was 2.25 V but at a sweep rate of 100 mV s^{-1} this decreased to 1.9 V. Because further experiments determined that this shift could not be attributed to *IR* drop, the reaction must be extremely irreversible. Cyclic voltammograms were also obtained at 0 °C. In this case the reduction peak is much smaller and more symmetric (Fig. 3(B)), indicating that the reduction product is less soluble at this temperature; however, the passivating layer was still sufficiently soluble to have been mostly removed by the second cycle. The reduction reaction is definitely different using the $LiGaCl_4$ salt and Raman spectroscopy was used to try and identify the discharge products for the two salts.

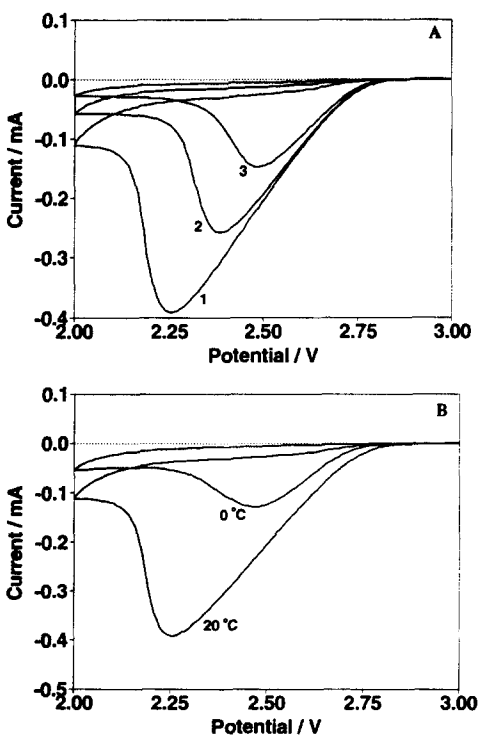

Fig. 3. Cyclic voltammograms obtained at a mechanically polished glassy-carbon electrode in $LiGaCl_4 \cdot 3.2SO_2$: (A) three consecutive cycles at 20 °C, and (B) first cycles at 20 and 0 °C (sweep rate = 10 mV s^{-1}).

3.2. *In situ pressure and Raman spectroscopic measurements during cell cycling*

A research cell was built that incorporated a pressure transducer, in order to record the pressure of SO_2 inside a cell during cycling. The voltage and pressure profiles of the cell were recorded when using the electrolyte $LiAlCl_4 \cdot 5.8SO_2$ at 22 °C and cycling between 2.7 and 4.0 V. During discharging the pressure was found to rise while during recharging the pressure fell again. This confirmed that $LiAlCl_4$ was being consumed during discharging, but not whether SO_2 was also being consumed in the proportion $LiAlCl_4$:$3SO_2$ to give the complex suggested by Dey et al. [4]. A very rough calculation was done to correlate the pressure change with changes in solution composition using Raoult's vapour pressure law, $p \propto (1 - X_B)$, where p is the vapour pressure of the solution and X_B is the mole fraction of solute. The calculation estimated that the salt and SO_2 were being consumed in the ratio of 1:4, respectively. Raoult's law should only be applied to dilute solutions so large errors will be present; however, the calculation indicates that SO_2 is also consumed during discharging. Raman spectroscopy was turned to as an alternative technique to measure changes in the composition of the electrolyte, by using the spectrum of SO_2 in the S–O symmetric stretching mode region. Two bands are seen in this region for the electrolyte $LiAlCl_4 \cdot 4SO_2$, see Fig. 4. The band at 1159 cm^{-1} arises from SO_2 that is solvated as $[Li(SO_2)_3]^+$ [10] while the band at 1146 cm^{-1} corresponds with that of pure liquid SO_2, which we loosely refer to as free SO_2. Discharging was carried out using a small cell consisting of a 30 mm long, 10 mm diameter glass tube with electrodes at either end, held in place by polytetrafluoroethylene connectors and Viton O-rings. Sufficient electrolyte was used in order to completely wet the carbon, separator and lithium. Excess electrolyte was avoided so that changes in the electrolyte composition would be discernible. In Fig. 4 it can be seen that the relative intensity of the band arising from fee SO_2 has increased during discharging. This shows that $LiAlCl_4$, or a $LiAlCl_4$:$3SO_2$ complex [4] is being consumed by the discharge reaction. When the experiment was repeated using $LiAlCl_4 \cdot 2.9SO_2$, very little change in the spectrum was observed; however, the 1146 cm^{-1} band did decrease rather than increase in relative intensity. This small decrease was a very good indication that $LiAlCl_4$:$3SO_2$

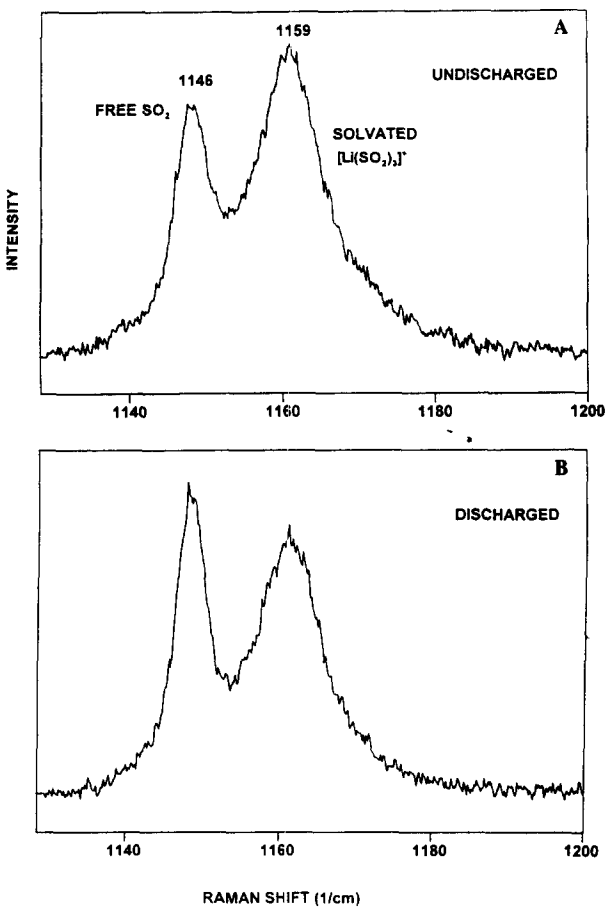

Fig. 4. In situ Raman spectra obtained from an $Li/LiAlCl_4 \cdot 4SO_2/C$ cell (A) before and (B) after discharging to 2.7 V; 457.9 nm excitation, 25 mW, 3 cm^{-1} band pass, and 4 s per point.

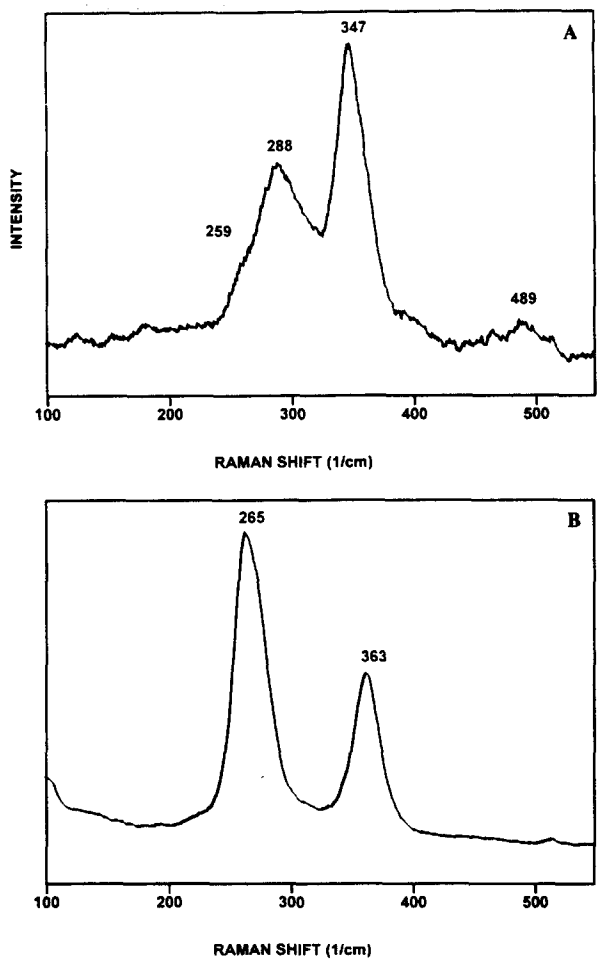

Fig. 5. Raman spectra obtained of Li/SO_2 cell discharge products: (A) in situ spectrum at the carbon electrode of the cell $Li/LiGaCl_4 \cdot 2.8SO_2/C$, and (B) ex situ spectrum of $Li_2S_2O_4$ on the surface of a carbon electrode taken from a discharged primary Li/SO_2 cell; 514.5 nm excitation, 15 mW, 32× microscope objective, 5 cm^{-1} bandpass, and 2 s per point.

was being consumed. A corresponding Raman experiment was carried out using $LiGaCl_4 \cdot 3.5SO_2$. In that case the band arising from free SO_2 fell in relative intensity during discharging, showing that SO_2 was consumed in the discharge reaction.

An attempt was made to identify the discharge products in the two cells. For the $LiAlCl_4 \cdot 4.0SO_2$ cell no new bands were detected, although LiCl, as a possible reduction product, does not yield a Raman spectrum. For $LiGaCl_4 \cdot 3.5SO_2$ (Fig. 5(A)), intense bands were found in the S–S stretching mode region, at 288 and 347 cm^{-1}, with weaker bands at 259 and 489 cm^{-1}. Crystalline $Li_2S_2O_4$ has two intense narrow Raman bands in this region, but the spectrum is otherwise quite different, see Fig. 5(B). The present spectrum may arise from a different isomorph of $Li_2S_2O_4$ or possibly from a complex such as $[GaCl_2(S_2O_4)]$. A more detailed study of this reduction product is in progress. This same species was also determined to be formed by corrosion of lithium metal in $LiGaCl_4 \cdot 3SO_2$ electrolyte. Corrosion in this electrolyte is much worse than in the $AlCl_4^-$-containing electrolyte and it is not suitable for use in a rechargeable lithium cell without an additive.

During the charging half of cell cycling, it is believed that the cell discharge products are chemically oxidised by chlorine that is produced from oxidation of $AlCl_4^-$ [8]. With constant current charging the voltage rises sharply near 4.0 V, when all the film has been oxidised and the observed overpotential is solely due to chlorine generation. During the subsequent discharge, chlorine that was not consumed in the charging process is seen to lead to an initially higher discharge voltage. Dey et al. [4] believed that the chlorine led to overcharge protection for the cell: Cl_2 diffused to the lithium electrode where it reacted to form LiCl, which then reacted with $AlCl_3$ in the electrolyte that had been co-produced with the Cl_2 (the $AlCl_3$ is actually present as $Al_2Cl_7^-$ ions, from reaction with $AlCl_4^-$).

When a glassy-carbon working electrode that has a reduction film on it is held at 4.0 V for a few minutes, the film is chemically removed by chlorine. Fig. 6(A) shows the voltammogram obtained after holding such

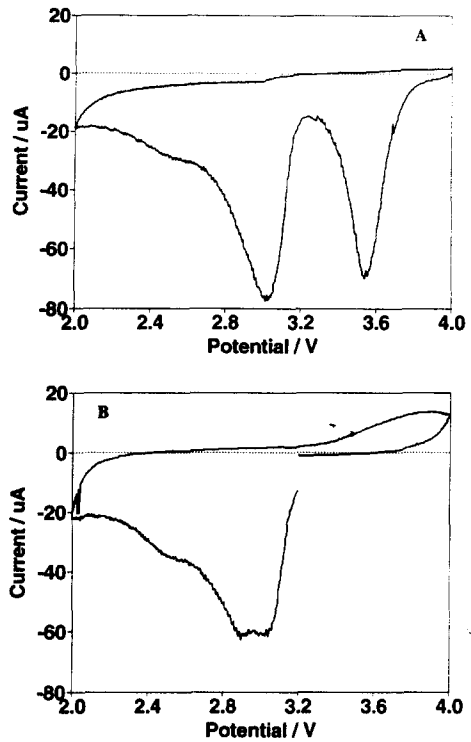

Fig. 6. Cyclic voltammograms obtained at previously cycled glassy-carbon electrodes following Cl_2 evolution at 4.0 V for 15 s: (A) cycle immediately started at 4.0 V, and (B) cycle started at 3.2 V within a few seconds of Cl_2 evolution; sweep rate = 100 mV s^{-1}.

an electrode for 15 s at 4.0 V and then immediately sweeping. A strong reduction peak is seen at 3.5 V. This peak disappears if the cell is left at open circuit for as little as 5 s before sweeping and arises from reduction of Cl_2 to LiCl [11]. The loss of this peak can be ascribed to a mixture of Cl_2 diffusion and reaction with SO_2 to produce SO_2Cl_2. The second reduction peak in Fig. 6(A) is at 3.0 V, rather than 2.9 V. SO_2Cl_2 dissolved in $LiAlCl_4 \cdot 3SO_2$ has been shown to have a reduction peak in this region that shifts from 3.0 to 3.2 V as the concentration is increased from 5×10^{-3} to 7.5×10^{-2} M using a platinum working electrode [12]. Therefore, the peak at 3.0 V is thought largely to arise from reduction of SO_2Cl_2 to LiCl and SO_2. Because of reduction of both Cl_2 and SO_2Cl_2, the carbon electrode was probably too passivated to allow much reduction of the bulk electrolyte to take place. In order to confirm this, the electrode was held at 4.0 V for 15 s and the sweep started at 3.2 V. In this case two reduction peaks were resolved, at 2.9 and 3.0 V (Fig. 6(B)) indicating that the thinner passivating film produced by reduction of SO_2Cl_2 at 3.0 V had allowed reduction of the electrolyte to take place at 2.9 V.

Raman spectroscopy was used to try and identify the species present in the electrolyte during Cl_2 evolution. A cell was constructed using a 5 mm diameter nuclear magnetic resonance tube, with a platinum electrode at the bottom and a lithium electrode at the top. The platinum electrode was held at 4.8 V and in situ Raman spectra were obtained with the laser beam parallel and close to its surface. The spectra obtained at various times are shown in Fig. 7. The electrolyte used was $(0.95\ NaAlCl_4, 0.05\ LiAlCl_4) \cdot 2.8SO_2$; sodium salt being used in order to reduce the possibility of overlapping

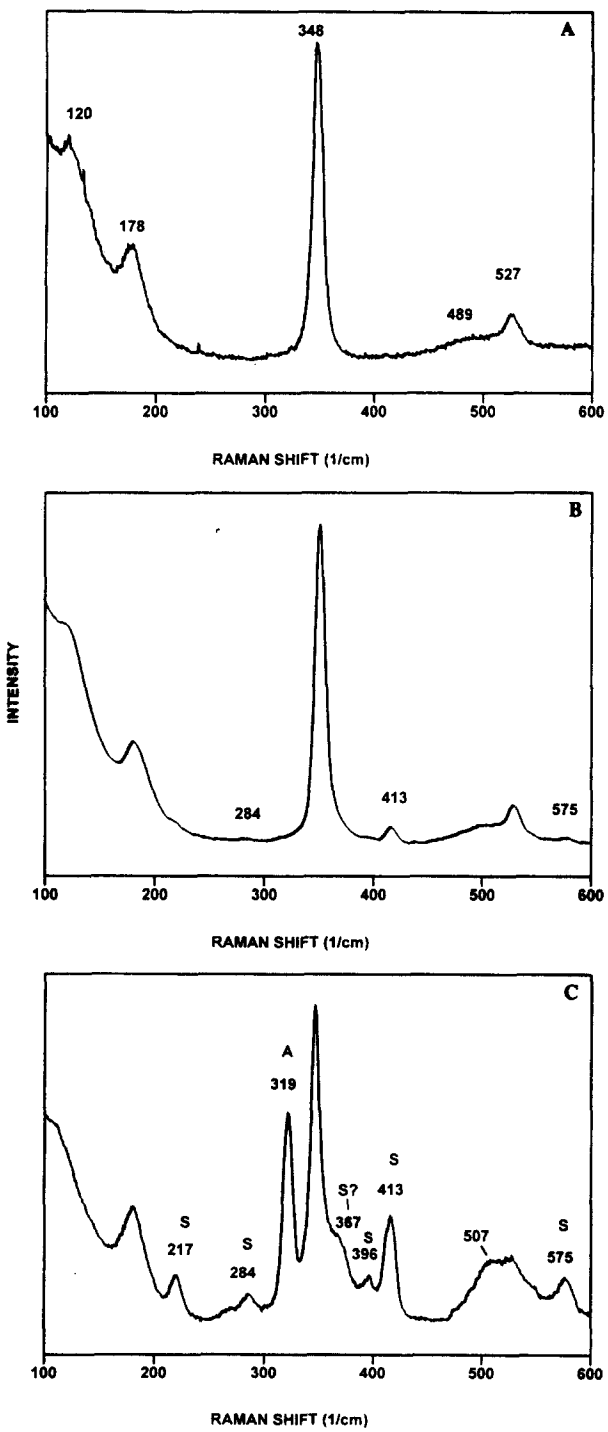

Fig. 7. In situ Raman spectra obtained for Cl_2 evolution at 4.8 V from a platinum electrode in $(0.95\ NaAlCl_4, 0.05\ LiAlCl_4) \cdot 2.8SO_2$: (A) fresh electrolyte, (B) after 2 h, and (C) after 20 h of Cl_2 evolution; 476.5 nm excitation, 50 mW, 4 cm^{-1} bandpass, and 4 s per point.

bands with SO_2Cl_2 in the O–S–O stretching mode region (the band maximum for the electrolyte is 1153 cm^{-1} and SO_2Cl_2 has a band at 1180 cm^{-1}). Fig. 7 shows the spectrum in the low frequency region where S–O bending and Al–Cl stretching and bending modes occur. The spectrum of the fresh electrolyte (Fig. 7(A)) is seen to change during Cl_2 evolution. No new bands could be detected at times of the order of a few minutes because of the weakness of the Raman effect, but results are shown following 2 h (Fig. 7(B)) and 20 h of Cl_2 evolution (Fig. 7(C)). New bands which can be assigned to expected species have been labelled in Fig. 7(C) where $A = Al_2Cl_7^-$ and $S = SO_2Cl_2$. Chlorine, present as an impurity in SO_2Cl_2, has a band at 554 cm^{-1}. No band is resolved in that region of the present spectra, although there may be a weak unresolved component. The reactions taking place at or near the platinum electrode are:

$$AlCl_4^- \longrightarrow AlCl_3 + 0.5Cl_2 + e^- \quad (1)$$

$$AlCl_3 + AlCl_4^- \longrightarrow Al_2Cl_7^- \quad (2)$$

and,

$$SO_2 + Cl_2 \rightleftharpoons SO_2Cl_2 \quad (3)$$

There are only two bands that cannot be accurately assigned. The first is at 367 cm^{-1} and the second at 507 cm^{-1}. The former band can be assigned as the SCl_2 antisymmetric stretching mode of SO_2Cl_2 [13], but it has a higher relative intensity than expected. The same applies to the broad band at 507 cm^{-1}. In this case $AlCl_4^-$ has an antisymmetric AlCl stretching mode 490 cm^{-1} [14]. One species that does have a Raman band in this region that could be present from a side reaction is SCl_2, which has an intense band at 514 cm^{-1} [15]. The Raman spectrum in the SO stretching mode region also changed during Cl_2 evolution. The band arising from free SO_2 increased in intensity and the symmetric SO stretching mode of SO_2Cl_2 appeared at 1180 cm^{-1}. The increased intensity of the free SO_2 band must be due to displacement of SO_2 from the solvation shell of the Na^+ by SO_2Cl_2.

In summary, during overcharging of an Li/$LiAlCl_4 \cdot xSO_2$/C cell, Cl_2 dissolves in the electrolyte and reacts to form SO_2Cl_2. Overcharge protection is still achieved in the same manner suggested by Dey et al. [4], because SO_2Cl_2 will attack Li to form LiCl which will be dissolved by $Al_2Cl_7^-$ species in the electrolyte.

4. Conclusions

The electrochemical reductions taking place at glassy-carbon electrodes in electrolytes of general formula $LiAlCl_4 \cdot xSO_4$ and $LiGaCl_4 \cdot xSO_2$ are markedly different. In the former case $LiAlCl_4{:}3SO_2$ is consumed and in the latter it is the SO_2. In situ Raman spectroscopy has shown that the reduction product in Ga-containing cells is not crystalline $Li_2S_2O_4$ as has been previously suggested and that chlorine produced during overcharging is converted to SO_2Cl_2. Cyclic voltammetry indicated that reaction of Cl_2 with SO_2 was rapid.

Acknowledgements

This work was carried out under contract to the Canadian Department of National Defence (Contract No. W2207-1-AF03).

References

[1] W.F. Meyers, B. Bell and J.W. Simmons, *US Patent No. 3 423 242* (1969).
[2] D.L. Maricle and J.P. Mohns, *US Patent No. 3 567 515* (1971).
[3] C.R. Schlaikjer, *US Patent No. 4 139 680* (1979).
[4] A.N. Dey, H.C. Kuo, P. Piliero and M. Kallianidis, *J. Electrochem. Soc., 135* (1988) 2115–2120.
[5] D.L. Foster, H.C. Huo, C.R. Schlaikjer and A.N. Dey, *J. Electrochem. Soc., 135* (1988) 2682–2686.
[6] H.C. Kuo, C.R. Schlaikjer, D. Foster, M. Kallianidis and A.N. Dey, in A.N. Dey (ed.), *Lithium Batteries,* Proc. Vol. 87-1, The Electrochemical Society, Pennington, NJ, USA, pp. 414–435.
[7] G.T.K. Fey, *J. Power Sources, 35* (1991) 153–162.
[8] R.J. Mammone and M. Binder, *J. Electrochem. Soc., 133* (1986) 1312–1315.
[9] T.J. Lee, G.T.K. Fey, P.C. Yao and S.Y. Chen, *J. Power Sources, 26* (1989) 511–517.
[10] M.C. Dhamelincourt, F. Wallart, P. Barbier and G. Mairesse, *J. Mol. Struct., 142* (1986) 463–466.
[11] E. Lojou, R. Messina, J. Perichon, J.P. Descroix and G. Sarre, *J. Electrochem. Soc., 136* (1989) 299–302.
[12] E. Lojou, R. Messina, J. Perichon, J.P. Descroix and G. Sarre, *J. Electrochem. Soc., 136* (1989) 293–298.
[13] R.J. Gillespie and E.A. Robinson, *Can. J. Chem., 39* (1961) 2171–2178.
[14] G. Torsi, G. Mamantov and G.M. Begun, *Inorg. Nucl. Chem. Lett., 6* (1970) 553–560.
[15] H. Stammreich, R. Forneris and K. Soret, *J. Chem. Phys., 23* (1955) 972–976.